Electronic Supplementary Material (ESI) for Physical Chemistry Chemical Physics.

# Supporting information

## Resonant Raman Spectra of Molecules with Diradical Character: Multiconfigurational Wavefunction Investigation of Neutral Viologens

Julia Romanova, Vincent Liégeois, and Benoît Champagne*

*Laboratoire de Chimie Théorique, Unité de Chimie Physique Théorique et Structurale (UCPTS),*
*University of Namur, Rue de Bruxelles 61, 5000 Namur, Belgium*

**Detailed analysis of Figure 1**

Within the *MP2 approach*, the most intensive peak is mainly associated with the 0-0 transition (FC factor = 2.51E-01). The fundamental vibrational excitations of modes 10 (FC 9.58E-02), 11 (FC 2.26E-02), and 29 (FC 4.31E-02), as well as the overtone $2\nu_{10}$ (FC 1.82E-02) also contribute this vibronic band. The peak at 378 nm represents the second most significant peak in the spectrum and its intensity is very close to the absorption maximum. This vibronic band mainly originated from the fundamental excitations of modes 63 (FC 8.51E-02) and 60 (FC 2.36E-02) and the simultaneous excitation of modes $\nu_{10}+\nu_{63}$ (FC 3.24E-02). The next important contributions to the second peak come from the fundamental excitations of modes 34 (FC 2.08E-02), 39 (FC 1.54E-02), and 43 (FC 1.92E-02), but also from the combinations of bands $\nu_{10}+\nu_{29}$ (FC 1.64E-02) and $\nu_{29}+\nu_{63}$ (FC 1.46E-02). The shoulder at 350 nm is associated mostly with the overtone $2\nu_{63}$ (FC 1.44E-02) but also with several combinations of bands: $\nu_{60}+\nu_{63}$ (FC 7.99E-03), $\nu_{10}+2\nu_{63}$ (FC 5.48E-03) and $\nu_{10}+\nu_{60}+\nu_{63}$ (FC 3.05E-03).

Within the *CASSCF approach*, the single vibronic band peaking at 378 nm originates from the 0-0 transition (FC 1.22 E-01) as well as from fundamental excitations of modes 29 (FC 8.92E-02), 63 (FC 3.19E-02), 10 (FC 2.54E-02), 46 (FC 2.24 E-02) and from the overtone $2\nu_{29}$ (FC 3.27E-02).

**Table S1.** Optimized bond lengths, R [Å] and dihedral angles θ [°] for the ground state of methyl viologen in different oxidation states as determined at different levels of approximation.

| | $MV^0$ | $MV^0$ | $MV^{2+}$ | $MV^{\bullet+}$ | $MV^0$ |
|---|---|---|---|---|---|
| | SS-CASSCF (14,12) | SS-CASSCF (10,10) | MP2 | MP2 | MP2 |
| $R(Me\text{-}N^1)$ | 1.446 | 1.446 | 1.491 | 1.469 | 1.456 |
| $R(N^1\text{-}C^1)$ | 1.391 | 1.395 | 1.355 | 1.368 | 1.393 |
| $R(C^1\text{-}C^2)$ | 1.350 | 1.349 | 1.390 | 1.373 | 1.362 |
| $R(C^2\text{-}C^3)$ | 1.467 | 1.469 | 1.403 | 1.429 | 1.453 |
| $R(C^3\text{-}C^{3'})$ | 1.374 | 1.372 | 1.482 | 1.433 | 1.391 |

**Table S2**. SA2-CASSCF vertical excitation energy $E_{0e}$ [eV], wavelength $\lambda_{0e}$ [nm] and transition dipole moment $\mu_{0e}$ [a.u.] of $PEV^0$. The SA2-CASPT2 values of $PEV^0$ are obtained by correcting the SA2-CASPT2 results of $MV^0$ for the effect of the phenylene extension, as determined at the SA2-CASSCF level [$\Delta E_{phenylene} = 4.68(PEV^0) - 5.65(MV^0) = -0.97$ eV].

| | SA2-CASSCF | SA2-CASPT2 |
|---|---|---|
| $E_{0e}$ | 4.68 | 2.31$^\dagger$ |
| $\lambda$ | 265 | 537 |
| $\mu$ | 4.23$^\dagger$ | |

$^\dagger$ Used for the simulations of RR and absorption spectra.

**Table S3.** Mode labels, vibrational frequencies $\omega_\ell$ [$\mathrm{cm}^{-1}$], and Huang-Rhys factors $S_\ell$ for the 1st excited state of $\mathrm{MV}^0$ and $\mathrm{PEV}^0$ calculated with the MP2 and SS-CASSCF methods. Only the normal modes with $S_\ell > 0.005$ are displayed.

| $\mathrm{MV}^0$ | | | | $\mathrm{PEV}^0$ | |
|---|---|---|---|---|---|
| MP2 | | SS-CASSCF | | MP2 | |
| $\omega_{\mathrm{sc.*}}$ | $S_\ell$ | $\omega_{\mathrm{sc.*}}$ | $S_\ell$ | $\omega_{\mathrm{sc.*}}$ | $S_\ell$ |
| 241 | 0.393 | 270 | 0.035 | 58 | 0.025 |
| 277 | 0.093 | 291 | 0.229 | 63 | 0.032 |
| 469 | 0.018 | 652 | 0.172 | 70 | 0.188 |
| 668 | 0.012 | 766 | 0.803 | 109 | 0.317 |
| 791 | 0.177 | 852 | 0.020 | 218 | 0.132 |
| 812 | 0.008 | 976 | 0.124 | 268 | 0.449 |
| 994 | 0.085 | 1139 | 0.042 | 293 | 0.008 |
| 1133 | 0.063 | 1200 | 0.080 | 335 | 0.738 |
| 1215 | 0.079 | 1245 | 0.202 | 384 | 0.007 |
| 1254 | 0.028 | 1467 | 0.027 | 390 | 0.014 |
| 1389 | 0.010 | 1489 | 0.008 | 418 | 0.012 |
| 1451 | 0.007 | 1548 | 0.150 | 431 | 0.136 |
| 1545 | 0.097 | 1659 | 0.287 | 492 | 0.098 |
| 1660 | 0.349 | | | 536 | 0.019 |
| | | | | 570 | 0.007 |
| | | | | 743 | 0.074 |
| | | | | 947 | 0.063 |
| | | | | 987 | 0.120 |
| | | | | 998 | 0.015 |
| | | | | 1234 | 0.154 |
| | | | | 1363 | 0.066 |
| | | | | 1472 | 0.108 |
| | | | | 1487 | 0.009 |
| | | | | 1565 | 0.107 |
| | | | | 1658 | 0.168 |

* Scaling factor 0.970

**Scaling factor 0.912

**Figure S1.** Initial guess for CASSCF calculation on $MV^0$ (right) and $PEV^0$ (left). The molecular symmetry of $PEV^0$ and $MV^0$ is $C_{2v}$ obtained with the RHF/STO-3G method.

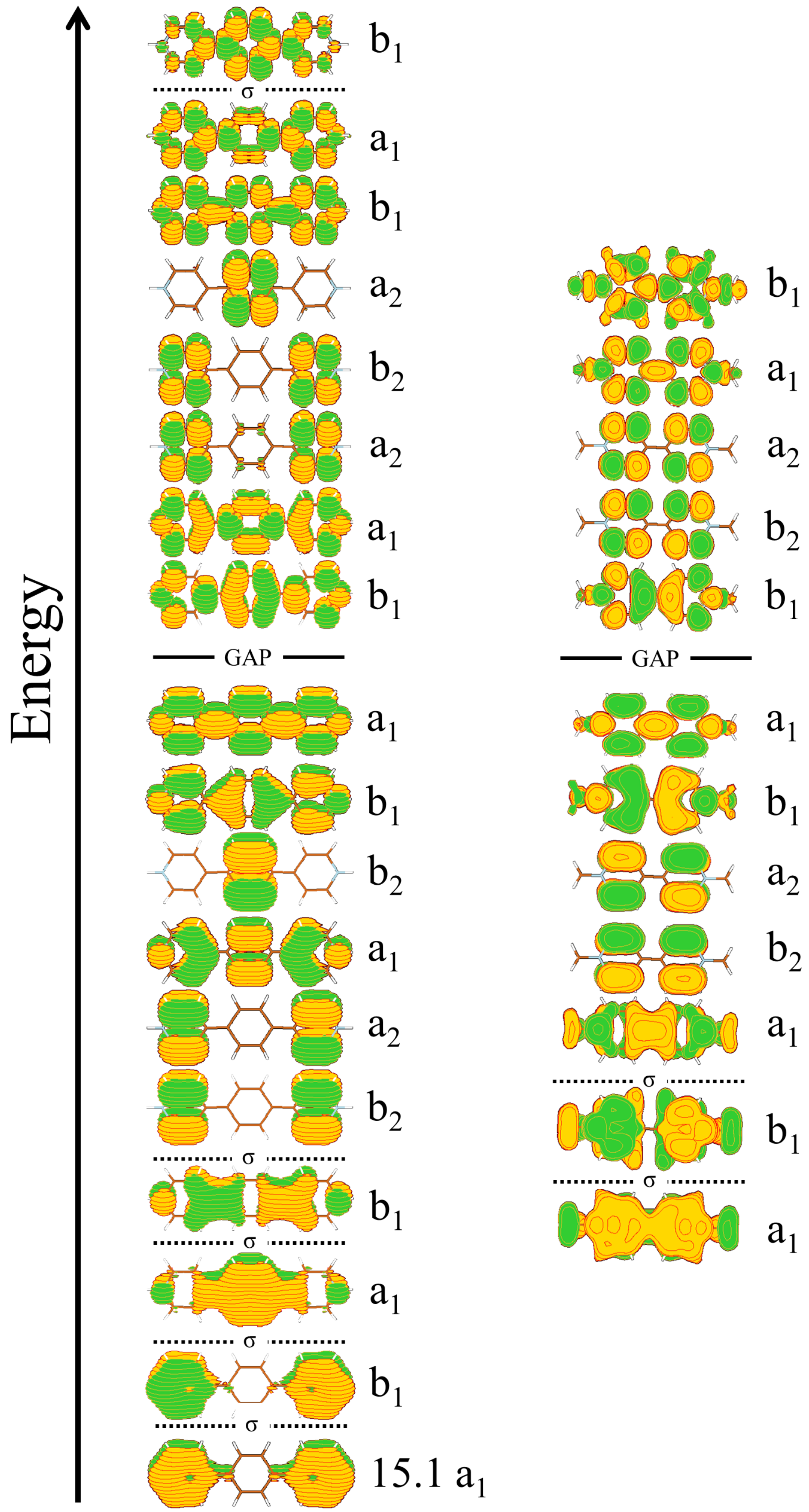

**Natural orbitals occupation numbers (ON) from SS-CASSCF(10,10) calculation on the MV$^0$ ground state:**

3 MOs in $a_1$ (16, ON=1.95; 17, ON=1.85; 18, ON=0.06)

3 MOs in $b_1$ (15, ON=1.93; 16, ON=0.13; 17, ON=0.04)

2 MOs in $b_2$ (9, ON=1.92; 10, ON=0.08)

2 MOs in $a_2$ (9, ON=1.92; 10, ON=0.08).

**Natural orbitals occupation numbers (ON) from SA2-CASSCF(10,10) calculation on the MV$^0$:**

3 MOs in $a_1$ (16, ON=1.96; 17, ON=1.42; 18, ON=0.06)

3 MOs in $b_1$ (15, ON=1.93; 16, ON=0.56; 17, ON=0.03)

2 MOs in $b_2$ (9, ON=1.92; 10, ON=0.08)

2 MOs in $a_2$ (9, ON=1.92; 10, ON=0.08).

**Major contributions in the CI vectors from SA2-CASSCF(10,10) calculation on the MV$^0$:**

$S_0$
22222 00000   0.90
22220 20000  -0.16

$S_1$
2222a b0000  -0.65
2222b a0000   0.65

**Natural orbitals occupation numbers (ON) from SS-CASSCF(16,16) calculation on the PEV$^0$ ground state:**

5 MOs in $a_1$ (17, ON=1.96; 19, ON=1.93; 20, ON=1.77; 21, ON=0.10; 22, ON=0.05)

5 MOs in $b_1$ (17, ON=1.95; 18, ON=1.90; 19, ON=0.23; 20, ON=0.06; 22, ON=0.04)

3 MOs in $b_2$ (12, ON=1.92; 13, ON=1.91; 14, ON=0.09)

3 MOs in $a_2$ (11, ON=1.92; 12, ON=0.09; 13, ON=0.09).

**Natural orbitals occupation numbers (ON) from SA2-CASSCF(16,16) calculation on the PEV$^0$:**

5 MOs in $a_1$ (17, ON=1.96; 19, ON=1.94; 20, ON=1.36; 21, ON=0.11; 22, ON=0.04)

5 MOs in $b_1$ (17, ON=1.95; 18, ON=1.91; 19, ON=0.62; 20, ON=0.06; 22, ON=0.03)

3 MOs in $b_2$ (12, ON=1.92; 13, ON=1.92; 14, ON=0.09)

3 MOs in $a_2$ (11, ON=1.92; 12, ON=0.09; 13, ON=0.08).

**Major contributions in the CI vectors from SA2-CASSCF(16,16) calculation on the PEV$^0$:**

$S_0$

| | |
|---|---|
| 22200 220 22000 200 | 0.814 |
| 22000 220 22200 200 | -0.214 |

$S_1$

| | |
|---|---|
| 22b00 220 22a00 200 | -0.607 |
| 22a00 220 22b00 200 | 0.607 |

**Figure S2.** $MV^{+\bullet}$ (left) and $MV^0$ (right) UV/vis absorption spectra from T. M. Bockman and J. K. Kochi, *J. Org. Chem.*, 1990, **55**, 4127.

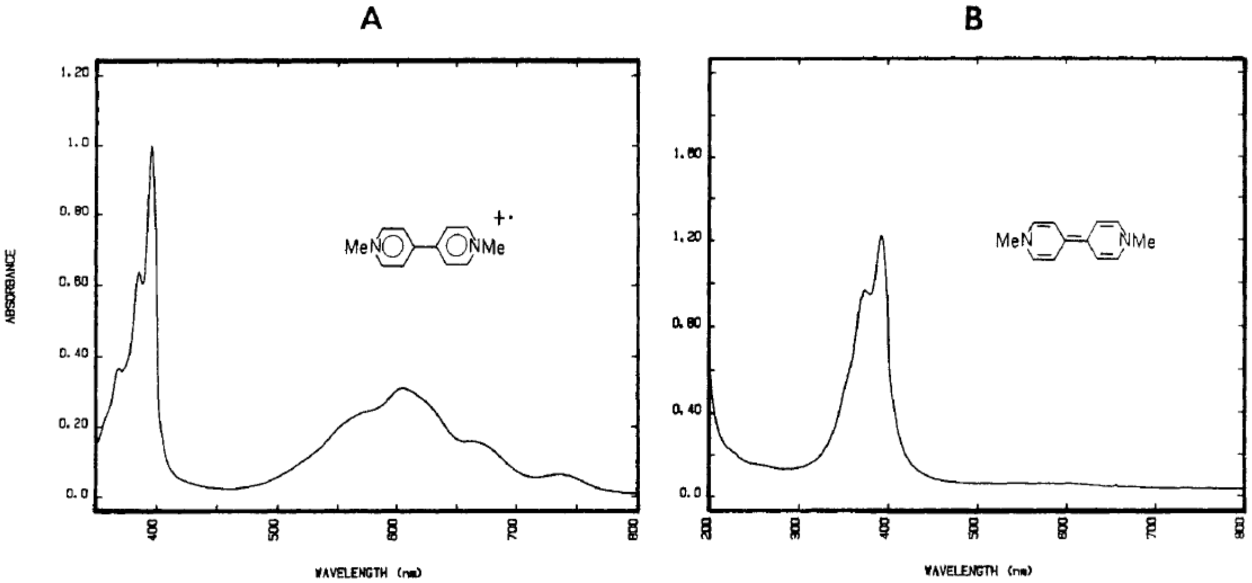

**Figure 1.** Absorption spectrum of (A) $5 \times 10^{-5}$ M $MV^{\bullet+}PF_6^-$ and (B) $3 \times 10^{-4}$ M $MV^0$ in dichloromethane.

**Figure S3. (Top)** RR spectra of $MV^0$ simulated by using SA2-CASSCF ground and excited state geometries together with MP2 (A) and SS-CASSCF (B) ground state vibrational normal modes. The energy of the incident light was to $E_{0e}$+0.30 eV in order to match the experimental 363.8 nm wavelength. The Raman bands are represented by Lorentzian functions with FWHM set to 10 $cm^{-1}$. **(Bottom)** Experimental RR spectrum of MV in different oxidation states. (d) corresponds to the RR spectrum of $MV^0$ prepared by electrolysis in acetonitrile solution, recorded at exciting laser wavelength 363.8 nm from Q. Feng and T. M. Cotton, *J. Phys. Chem.*, 1986, **90**, 983.

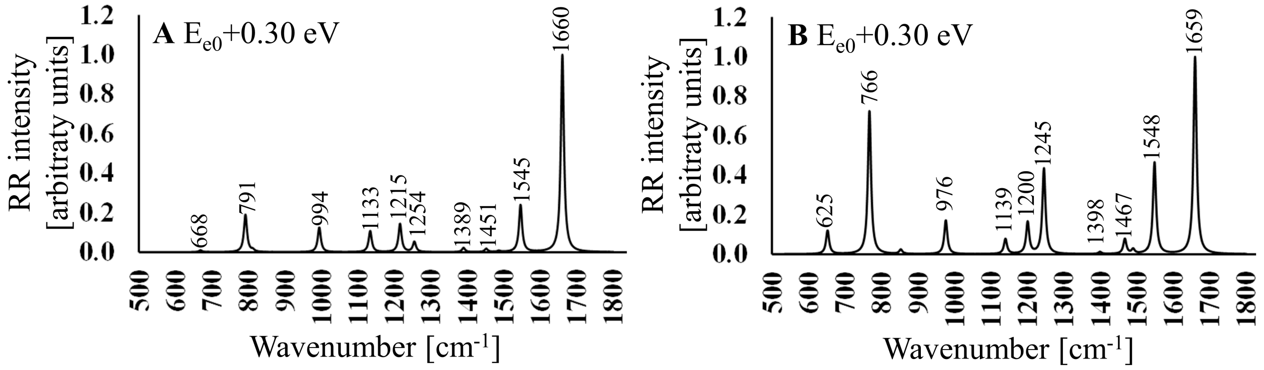

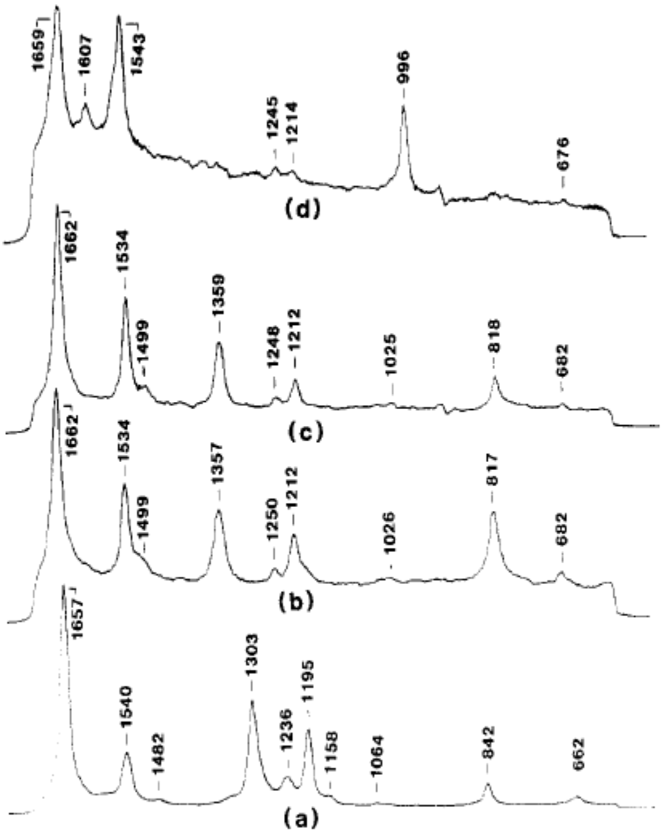

**Figure 1.** Raman scattering spectra of (a) 0.1 M $MV^{2+}$ in aqueous solution; (b) $MV^{+\cdot}$ in aqueous solution, prepared by reacting 1 mM $MV^{2+}$ with $Na_2S_2O_4$; (c) $MV^{+\cdot}$ prepared by electrolysis of 0.25 mM $MV^{2+}$ in acetonitrile; (d) $MV^0$ prepared by further electrolysis of c. Exciting laser wavelength 363.8 nm; power 30 mW. The acetonitrile spectrum was subtracted from c and d.